J. Mol. Biol. (1984) **179**, 55–81

Microsecond Rotational Motions of Eosin-labeled Myosin Measured by Time-resolved Anisotropy of Absorption and Phosphorescence

THOMAS M. EADS†, DAVID D. THOMAS‡

Department of Biochemistry
University of Minnesota Medical School
Minneapolis, MN 55455, U.S.A.

AND

ROBERT H. AUSTIN

Department of Physics, Princeton University
Princeton, NJ 08544, U.S.A.

(Received 2 November 1983, and in revised form 3 April 1984)

We have studied submicrosecond and microsecond rotational motions within the contractile protein myosin by observing the time-resolved anisotropy of both absorption and emission from the long-lived triplet state of eosin-5-iodoacetamide covalently bound to a specific site on the myosin head. These results, reporting anisotropy data up to 50 microseconds after excitation, extend by two orders of magnitude the time range of data on time-resolved site-specific probe motion in myosin. Optical and enzymatic analyses of the labeled myosin and its chymotryptic digests show that more than 95% of the probe is specifically attached to sulfhydryl-1 (SH_1) on the myosin head. In a solution of labeled subfragment-1 (S-1) at 4°C, absorption anisotropy at 0·1 μs after a laser pulse is about 0·27. This anisotropy decays exponentially with a rotational correlation time of 210 ns, in good agreement with the theoretical prediction for end-over-end tumbling of S-1, and with times determined previously by fluorescence and electron paramagnetic resonance. In aqueous glycerol solutions, this correlation time is proportional to viscosity/temperature in the microsecond time range. Furthermore, binding to actin greatly restricts probe motion. Thus the bound eosin is a reliable probe of myosin-head rotational motion in the submicrosecond and microsecond time ranges. Our submicrosecond data for myosin monomers (correlation time 400 ns) also agree with previous results using other techniques, but we also detect a previously unresolvable slower decay component (correlation time 2·6 μs), indicating that the faster motions are restricted in amplitude. This restriction is not consistent with the commonly accepted free-swivel model of S-1 attachment in myosin. In synthetic thick filaments of myosin, both fast (700 ns) and slow (5 μs) components of anisotropy decay are observed. In contrast to the data for monomers, the anisotropy of filaments has a substantial residual component (26% of the initial anisotropy) that does not decay to zero even at

† Present address: Department of Chemistry, University of Minnesota, Minneapolis, MN 55455, U.S.A.

‡ Author to whom correspondence should be addressed.

0022–2836/84/290055–27 $03.00/0

times as long as 50 μs, implying significant restriction in overall rotational amplitude. This result is consistent with motion restricted to a cone half-angle of about 50°. The combined results are consistent with a model in which myosin has two principal sites of segmental flexibility, one giving rise to submicrosecond motions (possibly corresponding to the junction between S-1 and S-2) and the other giving rise to microsecond motions (possibly corresponding to the junction between S-2 and light meromyosin). Both motions are slower and more restricted in filaments than in monomers. This study complements previous fluorescence and electron paramagnetic resonance studies by extending the time range and providing time-resolution, respectively, thus providing a more complete description of myosin rotational dynamics.

1. Introduction

Several major features of muscle contractile systems have been described with adequate detail to allow models for the mechanism to be developed and tested. The question addressed most often, either explicitly or implicitly, by recent research is: what is the nature of the (anisotropic) changes in macromolecular dimensions that must accompany the macroscopic change in length and the development of tension? It is frequently proposed that some parts of the actin and myosin molecules are the sites of the mechanochemical process that generates force during contraction. Many studies have addressed the hypothesis that *rotational* motions within myosin are coupled to force generation (Huxley, 1969). While it is important to test particular features of this model, it is also necessary to investigate structural fluctuations from the phenomenological point of view, since the physiological transitions that occur during contraction probably involve complex changes in the state of motion of contractile proteins.

Two sites in myosin have properties that suggest they can act as "hinges" about which large-scale rotations might occur: the region that joins each of the two globular myosin heads (designated "subfragment-1" or "S-1" when prepared as the proteolytic fragment) to the fibrous tail (designated "myosin rod"), and the region near the middle of rod between subfragment-2 and light meromyosin, the part of myosin rod that forms the backbone of the myosin filament. The points of flexibility were first identified as regions of proteolytic susceptibility (Lowey *et al.*, 1969). In addition to large-scale rotations, there are also internal motions characteristic of parts of the molecule (globular and fibrous).

Several physical methods that measure rotational relaxation indicate that motions in myosin have time constants covering a range from nanoseconds to milliseconds. Nuclear magnetic resonance results suggested nanosecond internal rotational motions of some hydrogen atoms (Highsmith *et al.*, 1982) and nanosecond to microsecond motions of backbone and side-chain carbon atoms (Eads, 1982; Eads & Mandelkern, 1984) within myosin. Microsecond fluctuatoons were indicated by viscoelastic measurements on rod (Hvidt *et al.*, 1982), depolarized light scattering of rod (Highsmith *et al.*, 1982), and electric birefringence of myosin (Bernengo & Cardinaud, 1982). Time-resolved X-ray diffraction measurements of positional (not necessarily rotational) fluctuations have shown that motions in the millisecond range are associated with the development of tension (Huxley, 1975; Huxley & Haselgrove, 1976; Yagi *et*

al., 1981; Huxley *et al.*, 1982). Among all of these results, reporting intrinsic molecular properties, it is often not clear which are the molecular domains that give rise to the signal or serve as scattering elements.

Site-specific molecular probes are essential for eliminating this ambiguity. For example, time-resolved fluorescence anisotropy of a probe bound covalently, specifically and rigidly to reactive cysteine SH_1† on the myosin head, made possible the direct measurement of the overall rotational motion of the head (Mendelson *et al.*, 1973,1975; Mendelson & Cheung, 1976,1978). Experiments with myosin monomers (i.e. at high ionic strength) suggested that the heads rotate in the nanosecond time-range relative to the rest of myosin. However, information in the microsecond range, which is essential for an unambiguous analysis of the data from the assembled myosin filament (i.e. at physiological ionic strength), was not obtainable. As previously discussed (Mendelson & Cheung, 1978; Thomas, 1978), the fluorescence method cannot provide this information, because of a fundamental limitation: the excited singlet state has a short lifetime (20 ns), resulting in unacceptably low signal-to-noise ratios in the anisotropy function after about 100 ns. In a complete experiment the anisotropy must have nearly completed its decay to provide sufficient information for analysis of amplitudes and rates of motion.

Sensitivity to microsecond rotational motions has been provided by saturation-transfer e.p.r. (Hyde & Thomas, 1980) studies of spin labels attached either to myosin heads or to actin (for reviews, see Thomas, 1978,1982). In the e.p.r. work, as in the fluorescence work, probes were selectively attached to SH_1 on the myosin head. e.p.r. studies on S-1 and myosin monomers confirmed the nanosecond motions previously observed by fluorescence, supporting the concept of a flexible myosin molecule (Thomas *et al.*, 1975*a*). The sensitivity of s.t.-e.p.r. to microsecond motion made possible a more complete study of myosin filaments, in which head motions were found to occur in a time range of 10 μs or less, depending on the pH and ionic strength (Thomas *et al.*, 1975*a*,*b*,1980). These motions are stopped (in the millisecond range) by F-actin (Thomas *et al.*, 1975*a*,1979). These e.p.r. studies were later extended to myofibrils and muscle fibers (Thomas *et al.*, 1980,1983; Thomas & Cooke, 1980; Cooke *et al.*, 1982). However, the e.p.r. method is not time-resolved, leaving ambiguity about details of the motions. For example, the question remains whether the longer effective correlation times in filaments and fibers are due to decreases in the rate or the amplitude of motions (or both) and whether there is more than one correlation time. This ambiguity might be resolved using time-resolved e.p.r., but the instrumentation is in its infancy and sensitivity is not yet sufficient for biological experiments.

The time-resolution capability and high sensitivity of optical anisotropy measurements can be exploited to study motion in the desired range (ns to ms) if optical probe molecules with very long excited-state lifetimes are used. This has

† Abbreviations used: S-1, proteolytic subfragment-1 (head of myosin; S-2, proteolytic subfragment-2 of myosin; SH_1, reactive cysteine in S-1; e.p.r., electron paramagnetic resonance: s.t.-e.p.r., saturation-transfer e.p.r.; E51A, eosin-5-iodoacetamide; EITC, eosin isothiocyanate; EGTA, ethylene glycol-bis-(β-aminoethylether)-*N*,*N*′-tetraacetic acid; MOPS, morpholinopropane sulfonic acid; EDTA, ethylenediaminetetraacetic acid; DTT, dithiothreitol; SDS, sodium dodecyl sulfate; PMSF, phenylmethylsulfonyl fluoride.

been done by a number of workers (for reviews, see Cherry, 1978; Jovin *et al.*, 1981), using probes such as eosin and erythrosin, which have stable triplet states that can be populated with high quantum efficiency. These states have microsecond to millisecond lifetimes, and so the anisotropy of the absorption or emission may be measured with good sensitivity over the entire time range to milliseconds.

In the present study, we have covalently and specifically attached an eosin derivative to SH_1 on the myosin head. We have measured the time-resolved anisotropy of absorption, and characterized quantitatively the amplitudes and rates of probe motion on myosin heads in the time range of nanoseconds to tens of microseconds.

2. Materials and Methods

(a) *Reagents*

Eosin-5-iodoacetamide was obtained from Molecular Probes, Inc. Eosin-Y (certified) was obtained from Kodak. Thin layer plates were Eastman Chromogram 13179. Sephadex was obtained from Pharmacia. Acrylamide/bis, 29 : 1, sodium dodecyl sulfate and TEMED were obtained from Biorad. α-Chymotrypsin (EC 3.4.21.1) type 1-S, glucose oxidase (EC 1.1.3.4) type IX, catalase and Coomassie Brilliant Blue R were obtained from Sigma. Coumarins were obtained from Exciton (Dayton, Ohio).

E5IA was stored at −20°C as a 8·31 mg/ml solution (approx. 10 mM, assuming that the powder received from the manufacturer is pure and anhydrous) in dimethyl formamide. The purity of stock solutions was periodically checked by thin-layer chromatography on silica gel plates, using 2 : 1 (v/v) benzene/methanol to elute. The extinction at 520 nm of a 0·0083 mg/ml aqueous solution of TLC-pure material was 0·95 cm^{-1}.

(b) *Preparation of proteins*

(i) *Myosin*

All operations were carried out at 4°C except where noted. Rabbit skeletal muscle myofibrils were prepared and glycerinated as described by Thomas *et al.* (1980). Myosin was prepared from glycerinated myofibrils as follows: to 1 vol. glycerinated myofibrils (25 mg/ml) was added 2 vol. rigor buffer (R buffer: 60 mM-KCl, 5 mM-$MgCl_2$, 1 mM-EGTA, 1 mM-NaN_3, 25 mM-MOPS, pH 7·0), the mixture was centrifuged at 1500 ***g*** for 10 min, and the pellet was resuspended to 25 mg/ml. To extract myosin, 0·146 vol. 2·5 M-KCl plus 0·02 vol. 0·1 M-ATP was added to bring the suspension to 0·37 M-KCl and 2 mM-ATP; the mixture was stirred gently for 15 min, then centrifuged at 40,000 ***g*** for 30 min. To the supernatant was added 8 vol. 0·1 mM-EDTA (pH 7·0) to precipitate myosin, which was collected by centrifugation at 10,000 ***g*** for 10 min. The concentration of myosin was determined (see below) and the pellet was brought to 25 mg/ml with 0·1 mM-EDTA. A second extraction was done by adding 0·24 vol. 2·5 M-KCl plus 0·005 vol. 1 M-$MgCl_2$, stirring, then adding 0·05 vol. 0·1 M-ATP, bringing the composition to 0·50 M-KCl, 5 mM-MgATP. This was immediately centrifuged at 100,000 ***g*** for 2 h. The supernatant, containing purified myosin, was diluted 2-fold and then glycerinated by dialysis overnight against 20 vol. storage buffer (50% (v/v) glycerol, 0·5 M-KCl, 0·5 mM-EDTA, 0·5 mM-DTT, 20 mM-MOPS, pH 7·0); this conveniently concentrates myosin by reducing the volume 3 or 4-fold. Glycerinated myosin was stored at −20°C. Myosin purity was estimated to be at least 95% as judged by SDS/polyacrylamide gel patterns, the principal contaminants being C-protein and actin.

(ii) *Chymotryptic subfragment-1 and rod*

Subfragment-1 was prepared from labeled and control myosin by a modification of the

method of Weeds & Taylor (1975). Myosin in M buffer (0·5 M-KCl, 10 mM-MOPS, 0·1 mM-EDTA, pH 7·0) at 5 mg/ml was dialyzed in F buffer (120 mM-KCl, 5 mM-$MgCl_2$, 1 mM-NaN_3, 1 mM-EGTA, 25 mM-MOPS, pH 7·0) to produce filaments. The suspension was brought to 20°C in a thermostatically controlled bath, then digested with α-chymotrypsin at a final concentration of 0·05 mg/ml (approx. 2·5 units/ml (Sigma)). The reaction was stirred continuously, and was stopped after 15 min by addition of 0·1 M-PMSF in ethanol to a final concentration of 1 mM. The mixture was dialyzed for 1 to 2 h against 200 vol. 0·1 mM-PMSF, 20 mM-MOPS (pH 7·0), at 4°C, and the precipitate (containing rod and undigested myosin) was pelleted by centrifugation at 30,000 ***g*** for 30 min. S-1 in the supernatant was purified by ammonium sulfate fractionation (Margossian & Lowey, 1973). Rod was purified by the method of Harrington & Burke (1972), except that the gel filtration and subsequent precipitation with ethanol was replaced by an ionic strength precipitation cycle. PMSF (0·1 mM) was used in all buffers subsequent to the dilution step. S-1 so prepared has intact heavy chains as judged by the SDS/polyacrylamide gel patterns. In addition to the main band at about $M_r = 100{,}000$, rod preparations showed faint bands indicative of contamination by light meromyosin, to the extent of 5 to 10%.

(c) *Labeling myosin with E5IA*

All operations involving eosin were carried out under dim red light to minimize photochemical modification of protein, and to reduce photolytic degradation of eosin-iodoacetamide. Glycerinated myosin was precipitated from storage buffer by dilution with 15 vol. water, and collected by centrifugation at 10,000 ***g*** for 20 min. The pellet was washed once with wash buffer (W buffer: 30 mM-KCl, 1 mM-EDTA, 10 mM-MOPS, pH 7·0), then dissolved to about 15 to 20 mg/ml with 500 mM-KCl, 1 mM-EDTA, 10 mM-MOPS (pH 7·0). Dissolved myosin was dialyzed at least 8 h in 100 vol. F buffer (pH 6·5) to form filaments. The pH was checked and adjusted if necessary. Myosin concentration was determined and adjusted, potassium pyrophosphate (PP_i) was added (from a 1 M stock solution), and the labeling reaction was started by adding E5IA (from a 10 mM stock solution in dialysis buffer plus 10% dimethylformamide). The labeling conditions used, unless otherwise stated, were as follows: 40 μM-myosin in F buffer plus 320 μM-E5IA, 4 mM-PP_i and 0·32% dimethylformamide, pH 6·5 (labeling time: 30 min). The reaction was stopped and filaments were dissolved in preparation for gel filtration by addition of 0·17 vol. 3·0 M-KCl, 14 mM-DTT, 10 mM-MOPS (pH 7·0) to produce a final composition of 0·62 M-KCl, 2·4 mM-DTT. Most unreacted and non-covalently bound dye was removed by gel filtration on a Sephadex G-25 column, eluted with 0·5 M-KCl, 2 mM-EDTA, 10 mM-MOPS (pH 7·0). Unreacted E5IA was bound (apparently irreversibly) to the top third of the column, and the purified pink conjugate was eluted in the void volume. It was pooled and dialyzed in 50 vol. 1 mM-EDTA, 10 mM-MOPS (pH 7·0) to precipitate myosin, which was collected by centrifugation at 10,000 ***g*** for 20 min; the pellet was dissolved by addition of an equal volume of 2 × M buffer, and brought to about 10 mg/ml by addition of M buffer. A final clarification was done by centrifuging at 40,000 ***g*** for 30 min. The product was either used immediately or glycerinated by addition of 1 vol. glycerol and then stored at −20°C. The control for this procedure was myosin, treated in the same way, except for the presence of E5IA.

The kinetics of myosin labeling were studied under varying reaction conditions. Samples were removed at various times, quenched as above and then run on individual small columns of Sephadex to remove unreacted dye. Samples were characterized by their dye/protein ratio and ATPase activities as described below.

(d) *Determination of labeling specificity*

(i) *Concentration of dye and protein*

The molar ratio of dye to protein was determined from the UV-VIS absorbance spectrum. Protein molar concentration was calculated from A_{280}, corrected for scattering

and for contribution at this wavelength from dye (determined in a separate experiment with pure dye of known concentration), and from the extinction coefficients for myosin ($E^{1\%}_{280} = 5{\cdot}5$, M_r 460,000; Godfrey & Harrington, 1970), or for S-1 ($E^{1\%}_{280} = 7{\cdot}5$, $M_r = 115{,}000$; Weeds & Pope, 1977), or rod ($E^{1\%}_{280} = 2{\cdot}0$, M_r 200,000; Harrington & Himmelfarb, 1972). The concentration of dye was determined from peak absorbance in the visible (near 530 nm), corrected for the 13% decrease in extinction on binding (determined in a separate experiment that measured the difference spectra of dye). Total eosin was corrected for non-covalently bound dye, which was estimated as follows: to 1·8 ml ethanol (95%, v/v, U.S.P.) at room temperature was added 0·2 ml of conjugate diluted to contain 1 to 10 μM dye. The mixture was mixed for 5 s, allowed to sit for 5 min, mixed 5 s, then centrifuged at about 3000 revs/min for 10 min. Control experiments showed that more than 90% of the protein was precipitated and more than 90% of the non-covalently bound dye was extracted. The supernatant fluorescence emission at 550 nm (excitation at 490 nm) was measured. Eosin in the supernatant was determined from a standard curve for E5IA in the same buffer as the conjugate, "extracted" as above. Two or three determinations were averaged. No more than 6% of the total eosin in Sephadex-diluted labeled myosin was extracted this way. This is an upper limit, since small amounts of unprecipitated labeled protein may have contributed to the supernatant fluorescence. Thus we estimate that at least 94% of eosin is covalently bound in these preparations. Extractable eosin on rod prepared from labeled myosin is only 0·2% of total eosin in labeled myosin. Thus most non-covalent dye is on the heads. Dye/protein ratios were typically 0·6 to 0·8 mol eosin/mol myosin.

(ii) *ATPase assay*

The steady-state rate of ATP hydrolysis by myosin was assayed at 25°C in the presence of high [K^+] and EDTA. The reaction mixture contained about 0·1 mg protein, 0·6 M-KCl, 5 mM-EDTA and 50 mM-MOPS (pH 7·5) in a volume of 1 ml. ATP was added to 5 mM, and samples were taken at 1-min intervals over a 5-min period. Quenching and measurement of inorganic phosphate (P_i) was based on the malachite green method of Lanzetta *et al.* (1979). Activities were calculated from the initial slope of the plot of P_i released *versus* time, and expressed as μmol P_i (mg protein)$^{-1}$ min^{-1}. The resulting measurement is designated K^+(EDTA)-ATPase activity, and the fractional inhibition of this activity (relative to unlabeled controls) is used as an estimate of the fraction of SH_1 groups that have been labeled (Kielley & Bradley, 1965; Yamaguchi & Sekine, 1966).

We defined the specificity parameter as the ratio of (the fractional inhibition in K^+(EDTA)-ATPase activity) to (dye molecules per myosin head). A value of 1·0 indicates specific labeling of SH_1, and a value less than 1·0 indicated the labeling of sites other than SH_1.

(iii) *Polyacrylamide gel electrophoresis*

A 3-level slab gel system similar to that of Ueno & Harrington (1981) was used. The bottom (middle) layers contained 13% (8%, w/v) acrylamide, 0·1% SDS, 0·375 M-Tris·HCl (pH 8·8), and the top layer (stacking gel) contained 4% acrylamide, 0·1% SDS, 0·125 M-Tris·HCl (pH 6·8). The weight ratio of acrylamide to bis(*N*,*N*-methylene bisacrylamide) was 29 : 1 in each. The running buffer was 0·1% SDS, 0·192 M-glycine, 0·25 M-Tris·HCl (pH 8·5). Samples were dissolved in 4 M-urea, 2% SDS, 10 mM-DTT, then heated at 80°C for 5 min just before loading onto gels. Electrophoresis at 25 mA per gel was carried out at a constant temperature of 20°C, using a Hoefer model SE600 system. Unstained, unfixed gels were backlit with ultraviolet light, and the fluorescence (filtered through yellow cellophane, so that only eosin was detected) was photographed on 4 inch × 5 inch film. The developed negatives were later scanned at 595 nm using the gel-scanning accessory on a Varian/Cary 210 spectrophotometer. The gels were stained with 1% Coomassie Brilliant Blue R in 50% (v/v) methanol, 7·5% acetic acid, and destained in 50% methanol, 7·5% acetic acid. The stained gels were cut into strips for densitometry. For gel loads in the range of 2 to 16 μg of protein, and for 3 to 12 pmol eosin, both the fluorescence and

Coomassie stain intensities determined by densitometry were linear. Dye/protein molar ratios for unknowns were determined from gels as follows: labeled protein of known concentration and dye content was electrophoresed at 3 or 4 loads, fluorescence and stain intensities were plotted as a function of moles of dye and protein, respectively, and slopes were determined. The dye and protein concentrations of an unknown run on the same gel were calculated by dividing observed intensities by the respective slopes. Owing to slightly different fluorescence and staining efficiencies, slopes differed among conjugates. Thus, for accurate results, an unknown had to be compared to a standard migrating at that position. In this way we measured the distribution of labeled products in chymotryptic digests of labeled myosin (see below) and in labeled glycerinated muscle fibers.

(e) *Oxygen removal*

We found that displacing oxygen by directing a stream of argon or nitrogen at the surface of a protein sample (Cherry, 1979) increased turbidity in solutions of myosin, filaments and S-1, and also produced longer correlation times and lower initial anisotropies in anisotropy experiments. Slower exchange by stirring under argon reduced, but did not eliminate, these problems. Rather, we employed two other methods. In the first, a protein sample was dialyzed overnight in a closed bath stirred by slow bubbling with argon. Subsequent handling was done in a glove bag, in an argon-filled basin, or under a gentle stream of gas. In the second method, an oxygen-consuming enzymatic reaction involving glucose oxidase and catalase was set up in the sample (see e.g. Horie & Vanderkooi, 1981). Lifetimes became maximal and stable about 20 min after addition of enzymes, at 4°C.

(f) *Spectroscopy*

(i) *Fluorescence and delayed luminescence spectra*

Steady-state fluorescence excitation and emission spectra and delayed luminescence spectra were obtained with a Spex Fluorolog 2 spectrofluorometer equipped with double monochromators for both excitation and emission. Emission spectra were not corrected for the variation of detector sensitivity with wavelength. The emission detector was a Hamamatsu R928 photomultiplier tube. Steady-state excitation was provided by a 450 W xenon-arc lamp. Delayed luminescence spectra were obtained by pulsed excitation with a xenon flash lamp; signal-gating circuitry allowed variable delay between a flash and the start of data acquisition as well as the length of time data was acquired after a flash. Signal averaging was employed in these experiments, and data files could be stored.

(ii) *Time-resolved emission spectrometer*

The apparatus is illustrated schematically in Fig. 1(b). Pulsed excitation of the dye laser was provided by a nitrogen laser (National Research Group 0·5-5-150/1B) with a pulse width of 5 ns. The dye laser (NRG DL-0·03) was operated either as a tuned (using a grating) or a broadband (using a mirror (m)) source, using Coumarin 485 or 500 (Exciton) at 10 mM in ethanol, to excite eosin in its visible absorption band near 520 nm. The sample and polarizing optics were contained in a box equipped for control of both temperature and atmosphere. The emission signal from the photomultiplier (PM) was electronically filtered to limit the bandwidth and reduce high-frequency noise, without disturbing the averaged decay curve. The signal was visualized on an oscilloscope, and digitized by a LeCroy 2256A 20 MHz waveform Digitizer (minimum period is 50 ns per point). 1000 to 10,000 transients were added and stored by a LeCroy 3500M multichannel analyzer.

Excitation was polarized vertically. Emission detected at 90° to the excitation beam passed through a polarizer oriented to analyze the components parallel ($I_{\parallel}$) and perpendicular ($I_{\perp}$) to the polarization axis of the excitation beam. This polarizer was rotated automatically every 50 or 100 pulses. Triplet emission in the red (phosphorescence) was isolated, and the contribution to the signal from scattering of pulsed excitation and from the eosin singlet emission band centered near 550 nm (prompt fluorescence) was

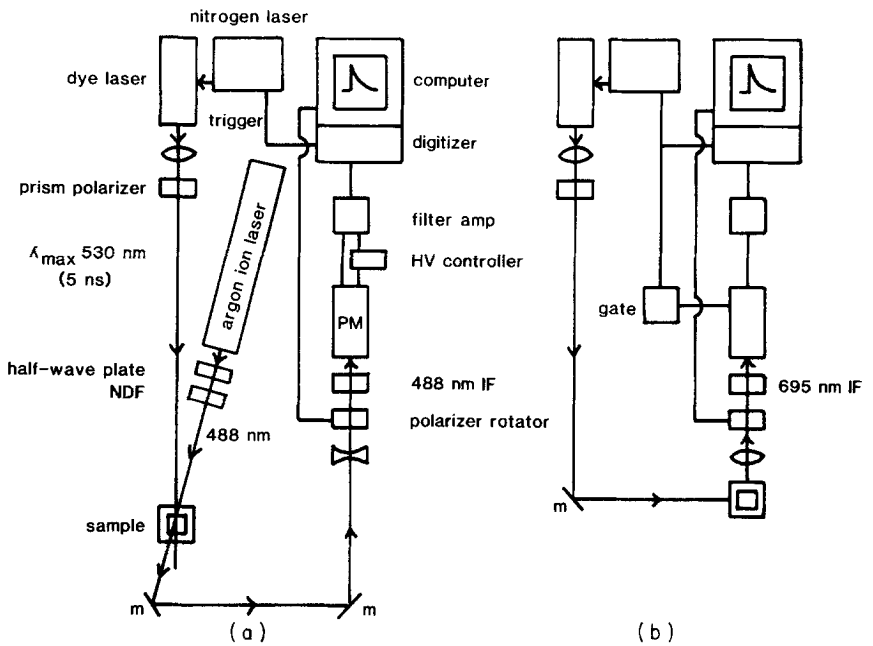

FIG. 1. Schematic drawing of the instrument used to measure time-resolved anisotropy of: (a) absorption and (b) the phosphorescence emission (University of Minnesota). Details are given in the text.

reduced using a 695±30 nm interference filter (IF; Spectrofilm, Inc.), and by gating the photomultiplier on at about 800 ns after the pulse. Excitation energy was typically 30 μJ/pulse in a 3 to 5 mm diameter beam, producing an energy density per pulse of about $1{\cdot}0\times10^{-4}$ to $2{\cdot}8\times10^{-4}$ J/cm^2. The record obtained with no light reaching the photomultiplier was subtracted to correct for small baseline distortions. The sum, corresponding to total luminescence decay, was calculated as: $S(t) = I_{\parallel}(t)+2kI_{\perp}(t)$. The anisotropy was calculated as: $r(t) = [I_{\parallel}(t)-kI_{\perp}(t)]/[I_{\parallel}(t)+2kI_{\perp}(t)]$. The factor k corrects for static contribution to anisotropy due to imperfections in emission side optics. Its value is determined as that required to give $r(t) = 0$ with a sample of eosin-Y in water. The value of k was typically 1·020 to 1·025.

(iii) *Time-resolved absorption spectrometer*

The apparatus used for experiments at the University of Minnesota is illustrated schematically in Fig. 1(a). We employed it for ground-state depletion experiments. Pulsed excitation in the green was provided by the nitrogen laser-pumped dye laser, operated in the broadband mode to produce maximum peak power. The pulse-induced depletion and regeneration of the ground singlet state was monitored by changes in absorption of a low-power (50 μW) continuous-wave probe beam at 488 nm from an argon-ion laser (Spectra-Physics 165), which was arranged to be very nearly colinear with the pulse beam within the cuvette. The sample was contained in a box equipped for control of temperature and atmosphere, and the sample could be stirred magnetically during experiments. The polarization of the probe beam was adjusted to give equal intensities for analyzer orientations parallel and perpendicular to the plane of excitation, by rotation of a half-wave plate. Fine control of the average (d.c.) signal level during experiments was obtained by electronically controlling the photomultiplier high voltage (HV) to produce a constant output. The controller was slow (0·5 s response time) and did not introduce artifacts into the very rapid (ms) polarized transmittance transients.

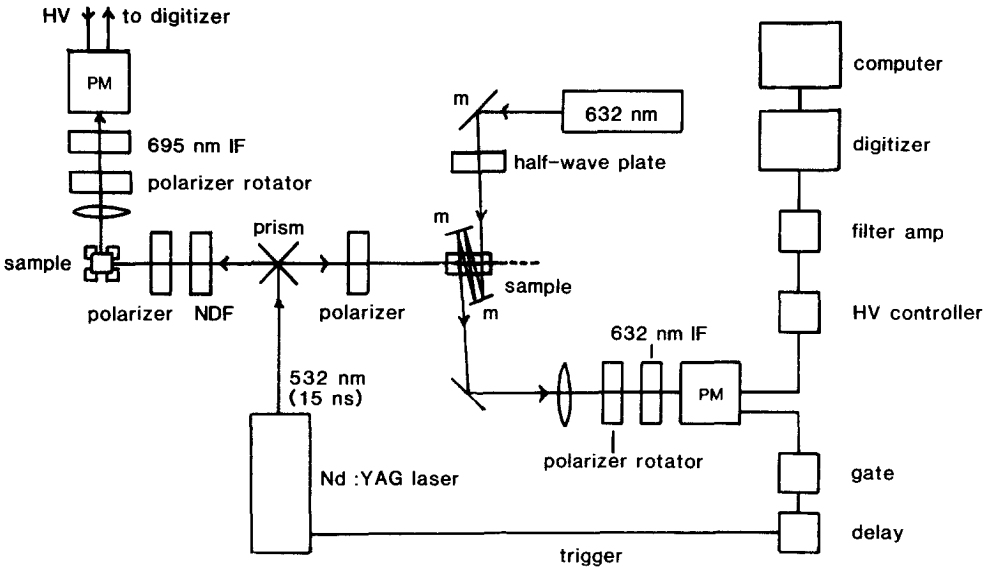

FIG. 2. Schematic drawing of the instrument used to measure time-resolved anistropy of absorption and of phosphorescence emission (Princeton University). The excitation beam was reflected at the prism either to the left (for emission) or to the right (for absorption).

The absorbance change $\Delta A(t)$ was calculated from intensity records obtained *with* ($I(t)$) and *without* ($I_0(t)$) pulsed excitation, obtained in separate runs on the same sample, as follows:

$$\Delta A_{\parallel}(t) = -\log \frac{I_{\parallel}(t)}{I_{0\parallel}(t)}, \qquad \Delta A_{\perp}(t) = -\log \frac{I_{\perp}(t)}{I_{0\perp}(t)}. \tag{1}$$

$I(t)$ was greater than $I_0(t)$ when the probe beam wavelength was in the singlet absorption band (green) corresponding to ground-state depletion; and $I(t)$ was less than $I_0(t)$ when the wavelength was in the triplet absorption band (red). Absorption sum and anisotropy were calculated as described for emission experiments, except that $k = 1$. The singlet absorption sum was inverted for display in the Figures.

The long path-length (about 2 m) from the probe beam to the sample effectively reduced the spike of scattered pulse radiation. Time resolution was limited by the shortest digitizer period of 50 ns per point; up to 1024 points could be obtained in a single transient.

Triplet absorption anisotropy experiments (absorption in the red) and some preliminary triplet emission experiments were performed at Princeton University on an instrument similar to that described previously (Austin *et al.*, 1979). Because of several modifications, the apparatus is shown in Fig. 2. The spectrometer at Princeton was used to obtain greater time resolution, so that the early part (2 to 100 ns) of the absorption anisotropy decay could be compared to the fluorescence emission results (Mendelson *et al.*, 1973).

(iv) *Statistical analysis of decay curves*

Decay curves (emission or absorption, sum or anisotropy) were analyzed by a least-squares fit of the data to the 1 or 2-exponential function:

$$A(t) = A_1 \exp(-t/\phi_1) + A_3 \tag{2}$$

$$A(t) = A_1 \exp(-t/\phi_1) + A_2 \exp(-t/\phi_2) + A_3. \tag{3}$$

The use of more complex functions (e.g. 3 exponentials) was not justified by the signal/noise. Equation (3) was used only if it resulted in a substantially better fit than

equation (2). Uncertainties were estimated by calculating standard deviations from several experiments on separate samples. Analysis in terms of specific molecular models is given in the Discussion.

3. Results

(a) *Extent and specificity of labeling*

We measured the kinetics of the reaction of myosin with eosin-5-iodoacetamide, in order to select conditions that maximized the extent and specificity of labeling a reactive cysteine group (SH_1) in the myosin head. We started with conditions that give good specificity with iodoacetamide analogs of nitroxide spin labels (Thomas *et al.*, 1980); namely, labeling myosin filaments at slightly acidic pH in the presence of magnesium pyrophosphate at 0°C. Then we varied pH, pyrophosphate concentration, and concentrations of reactants. Kinetics experiments were done and analyzed in terms of extent and specificity as described in Materials and Methods. The reaction of myosin with excess E5IA did not follow simple first-order kinetics, suggesting heterogeneous labeling, and specificity for SH_1 was high only at early reaction times, when less than half the SH_1 groups had reacted. This is in contrast to labeling with an iodoacetamide spin label, where excellent specificity is achieved after labeling virtually all of the SH_1 groups (Thomas *et al.*, 1980). We found that the following conditions gave the best specificity: 40 μM-myosin, 320 μM-eosin, 4 mM-pyrophosphate (pH 6·5) and short reaction time (0·5 h), the conditions described in Materials and Methods.

Some properties of eosin-labeled myosin are given in Table 1. Analysis of UV-VIS absorbance spectra of the Sephadex-purified conjugate indicated the presence of 0·7 to 0·8 labels per myosin molecule. Specificity of labeling was assessed by electrophoresis and ATPase assays. To view the distribution of label among the subunits of myosin, the conjugate was denatured in SDS and DTT, then electrophoresed on SDS/polyacrylamide gels. Eosin fluorescence in the unstained gel appeared in the heavy-chain band and not in the light-chain bands (Fig. 3). To view the distribution of label among the proteolytic fragments of myosin, the conjugate was digested with α-chymotrypsin under conditions favoring production of S-1 and rod. Samples were taken at various times, the reaction was quenched, run on SDS/polyacrylamide gels, photographed for ultraviolet light-induced fluorescence and then stained. Densitometry of negatives

TABLE 1

Specificity of labeling myosin SH_1 with eosin-5-iodoacetamide

ATPase activity				
Labeled (a)	Unlabeled (a°)	Fractional decrease in activity ($1-(a/a^\circ)$)	Dye/protein ratio (d/p)	Specificity $[1-(a/a^\circ)]/(d/p)$
1·62±0·11	2·47±0·18	0·34±0·13	0·36±0·02	0·96±0·18

K^+ (EDTA)-ATPase activities are expressed in μmol P_i (mg protein)$^{-1}$ min^{-1}. Dye/protein ratio is given as mol eosin per mol of heads (2 heads or 2 SH_1 groups per myosin). Uncertainties are given as the standard error of the mean, with $n = 4$ for activities and $n = 3$ for dye/protein ratios. The specificity is the ratio of the extent of ATPase inhibition (SH_1 blocking) to the extent of labeling.

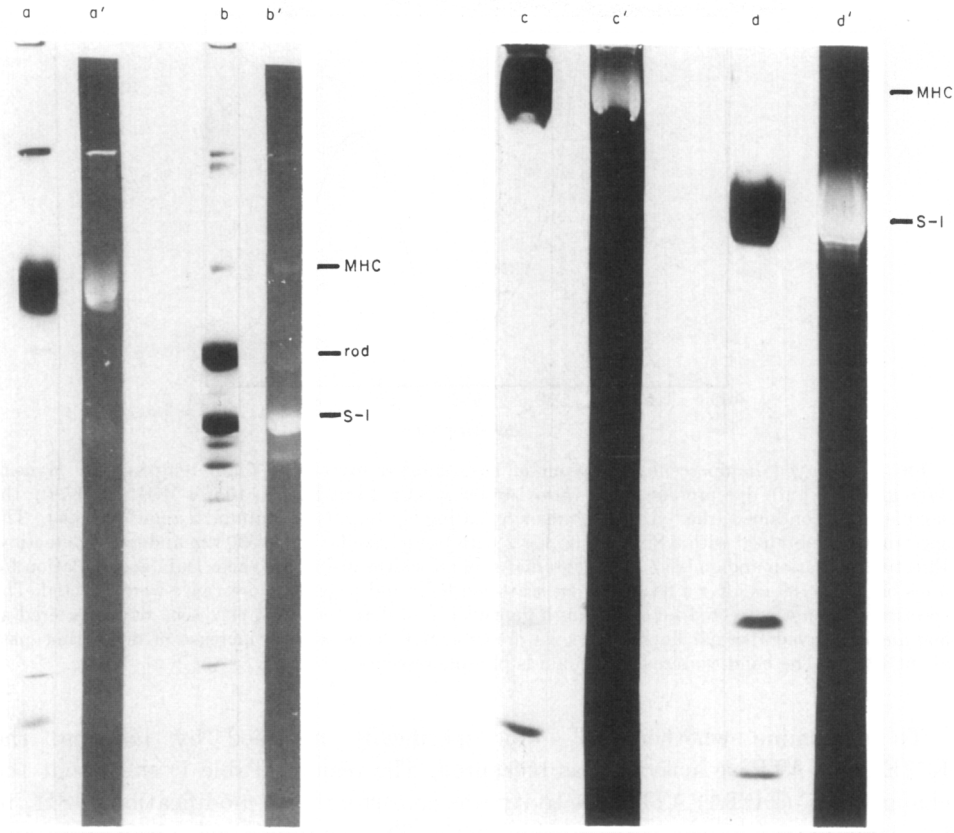

FIG. 3. Sodium dodecyl sulfate/polyacrylamide gel electrophoresis of eosin-labeled myosin and its chymotryptic digestion products. Lanes a to d, Coomassie Brilliant Blue-stained images; lanes a′ to d′, ultraviolet light-induced eosin fluorescence images (photographed before staining). Labeled protein was prepared, digested, electrophoresed and photographed as described in Materials and Methods. The position of myosin heavy chain (MHC), S-1 heavy chain (S-1), and rod were determined by running purified preparations of these proteins on the same slab gel. Lanes a and a′, eosin-labeled myosin (0·72 eosins per myosin); lanes b and b′, 5-min chymotryptic digest; lanes c and c′, eosin-labeled myosin run on a gradient gel; lanes d and d′, S-1 from a 15-min chymotryptic digest of the myosin in lane c, purified by ammonium sulfate fractionation. This labeled S-1 was also used in the experiments shown in Figs 7, 8 and 9.

showed that after five minutes of digestion, at least 85% of the dye associated with digestion products (excluding the undigested myosin heavy-chain band) was in the S-1 band, 0 to 10% was associated with the rod, and the remainder was in the low molecular weight digestion products. We purified rod from chymotryptic digests of labeled myosin and determined from absorbance measurements that $2{\cdot}3\% \pm 1\%$ of the total eosin was bound to the rod. Thus $97{\cdot}7\% \pm 1\%$ of the label is on the heads (S-1). Furthermore, the phosphorescence quantum yield for labeled rod was found to be no more than that of labeled S-1, implying that the label on rod contributes no more than $2{\cdot}3\% \pm 1\%$ to the total phosphorescence or transient absorption signal from labeled myosin.

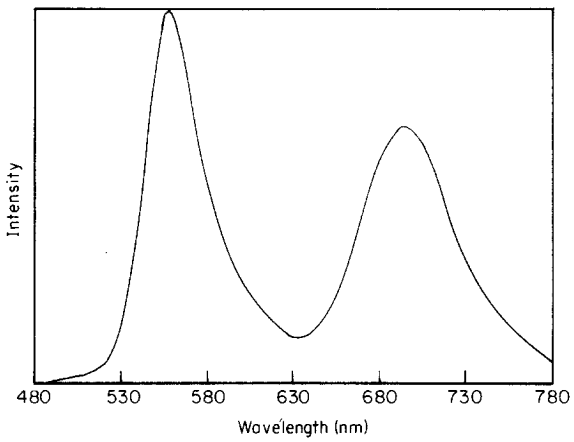

FIG. 4. Delayed luminescence spectrum of eosin-labeled myosin at room temperature. Myosin, 4·0 mg/ml (8·7 μm); dye/protein molar ratio 1·6; 0·5 M-KCl, 1 mM-EDTA, 10 mM-MOPS (pH 7·0); the sample also contained the enzymatic deoxygenating system (see Materials and Methods). The spectrum was obtained with a Spex Fluorolog 2 with pulsed excitation at 530 nm and gated detection. Effective excitation and emission monochromator band-widths are 14 nm each. Data accumulation for 5 ms began at 180 μs after a flash, so that scattered light and prompt fluorescence were rejected. The spectrum was not corrected for wavelength-dependence of detector sensitivity. The band centered at 560 nm is delayed thermal fluorescence; its area did not decrease with increase of delay time past about 120 μs. The band centered at 695 nm is phosphorescence.

To determine whether SH_1 was specifically modified by labeling, the K^+(EDTA)-ATPase activity was measured. The results (Table 1) show that the change in K^+(EDTA)-ATPase activity was consistent with modification of SH_1 to the same extent as the total labeling ratio. The combined gel, absorbance and ATPase results demonstrate that all of the label is on myosin heavy chain, most of it is on myosin head (S-1), no more than 2 to 3% is on myosin rod, and at least 78% (most probably 96%) is specifically and covalently bound to the reactive cysteine SH_1 on the head.

(b) *Steady-state spectroscopic properties of eosin covalently bound to myosin*

In the absorbance spectrum of the conjugate, the eosin peak in the visible region (530 nm) shifted to the red by about 12 nm relative to that of free dye, and the extinction coefficient at the wavelength of maximum absorbance decreased by about 13% relative to that of free dye. The fluorescence emission spectrum of the conjugate shifted toward the red by about 4 nm. The delayed luminescence spectrum of the E5IA–myosin conjugate is shown in Figure 4. This spectrum guided the selection of appropriate filters to isolate the emission band of interest in time-resolved optical measurements. In this case we chose the phosphorescence band. The spectral shifts suggest that eosin is in a hydrophobic environment when conjugated to myosin. This hypothesis is supported by the results in Figure 5 for phosphorescence emission lifetimes in air-saturated solutions of conjugate. Long lifetimes are in the range of hundreds of microseconds, much longer than that of

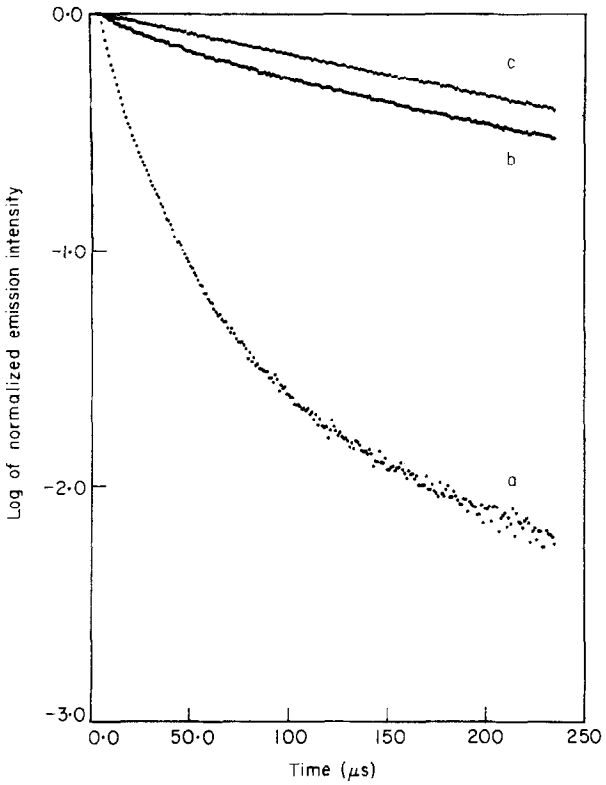

FIG. 5. Phosphorescence emission decay of eosin-labeled myosin. Intensities $[I_{\parallel}(t)]$ are normalized to the maximum of each and begin at 1 μs after the laser pulse. Excitation was at 530 nm; 1000 transients were averaged using the instrument in Fig. 1(b). Curve a, myosin, 2·8 mg/ml (6·2 μM); dye/protein molar ratio 0·8; 0·5 M-KCl, 5 mM-$MgCl_2$, 1 mM-EGTA, 1 mM-NaN_3, 25 mM-MOPS (pH 7·0), 4°C. Curve b, to the sample shown in curve a was added the enzymatic deoxygenating system (see Materials and Methods) (this addition diluted the sample to 1·15 vol.), the head space in the cuvette was flushed with argon, and allowed to stand for 30 min before the experiment. The sample was not stirred during data acquisition. Curve c, eosin, 1 μM in water, bubbled continuously with argon; emission lifetime, 580 μs.

free dye (4 μs, not shown), indicating that the probe is partially protected from quenching by dissolved oxygen. This was also observed for EITC–ovalbumin (Cherry *et al.*, 1976).

(c) *Lifetime experiments*

The decay of total emission intensity in the phosphorescence (red) band of eosin-labeled myosin monomers was multiexponential (Fig. 5, curve b), in contrast with the single exponential decay of the free dye (curve c). Similar multiexponential decays were seen for S-1 and filaments (data not shown). Multiple lifetimes could be related to ground-state heterogeneity; for example, impurity of the dye or lack of labeling site-specificity. However, (Fig. 5, curve a) the dye purity was ascertained to be quite high by thin-layer chromatography, and this was supported by the single-exponential phosphorescence decay of free

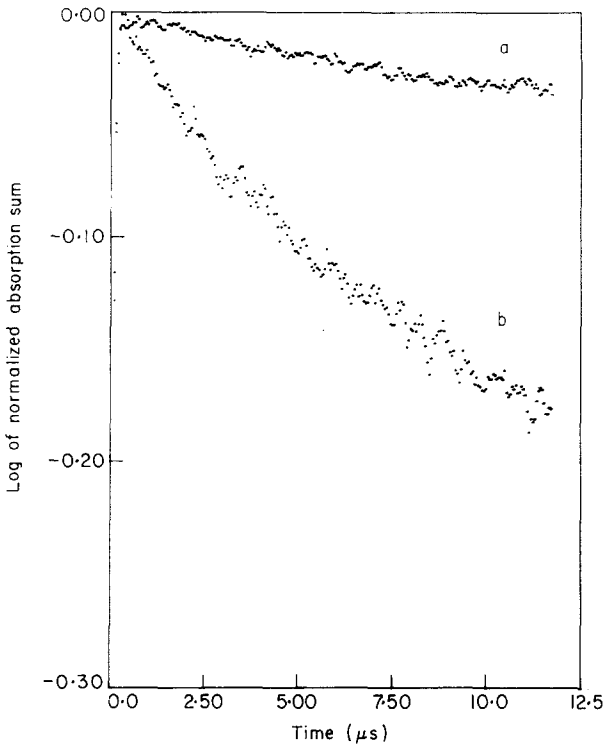

FIG. 6. Decay of the change in absorption (ground-state depletion) of eosin-labeled myosin. Records (absorption sum) are normalized to the maximum of each and begin 50 ns after the laser pulse. Broadband excitation was centered at 530 nm. Experiments were done at 4°C on the instrument shown in Fig. 1(a). Curve a, eosin-Y, 10 μM in water, continuous argon bubbling. Curve b, myosin, 28·3 μM (13 mg/ml); dye/protein molar ratio 0·72; solvent and enzyme composition as described in legend to Fig. 5. The sample was magnetically stirred at about 3 Hz during data acquisition; argon was maintained in the cuvette head space above the sample. Maximum absorbance change, ΔA, was 0·225 for 10 μM-eosin and 0·089 for 20 μM-eosin covalently bound to myosin. This myosin comes from the preparation characterized in Tables 1 and 2 and in Figs 8 and 9.

dye; curve b shows that labeling-site specificity for SH_1 was excellent, as discussed above. The complex emission decay may be due to microheterogeneity; for example, the SH_1-bound dye may have a distribution of states with different triplet-state lifetimes, corresponding to different local protein–dye bound conformations. If the conformational equilibrium is dynamic on the time scale of the excited-state lifetime, it may be possible to observe slow (submicrosecond to millisecond) conformational processes in myosin using the triplet analog of time-resolved emission spectroscopy (Badea & Brand, 1979; Brand *et al.*, 1981). The complex decay may also arise from excited-state reactions. For example, it is known that eosin can form semi-oxidized and semi-reduced species upon excitation in solution (Kasche & Lindquist, 1965) and that its photosensitizing properties are related to the reactions of its excited-state species with oxygen and with protein functional groups (Fisher *et al.*, 1976). (We have not seen significant changes in lifetime profiles of the eosin–myosin conjugate, even after lengthy exposure to pulsed excitation, so we have no spectroscopic evidence for

irreversible changes.) We also observe multiexponential decay of the absorbance change in the singlet band (see Fig. 6) and in the triplet–triplet absorption band (data not shown). (Note that the scales in Fig. 6 are greatly expanded relative to those of Fig. 5.) An adduct of *N*-(3-pyrene)-maleimide with myosin was also shown to have complex kinetics of emission from the first excited singlet state (Weltman *et al.*, 1973).

Multiexponential emission decays have been observed in a number of eosin systems: eosin–isothiocyanate in 80% glycerol, EITC–erythrocytes, EITC–concanavalin A (Austin *et al.*, 1979), and eosin-5-maleimide(E5M)–band 3 protein (Jovin *et al.*, 1981). Multiexponential absorbance changes were observed in EITC–ovalbumin and EITC–bovine serum albumin (Cherry *et al.*, 1976), and in EITC– and E5M–ATPase of sarcoplasmic reticulum (Burkli & Cherry, 1981) but not in a non-covalent eosin–albumin complex (Garland & Moore, 1979).

The presence of multiple lifetimes can complicate the analysis of anisotropy decay. Fuller examination of the errors associated with deriving rotational relaxation parameters from anisotropy curves that contain information about both level kinetics (lifetimes) and reorientation (correlation times) must await the application of newly developed theory (Cross *et al.*, 1983) to data on well-studied dye–protein conjugates. However, even the shortest components of triplet-state lifetimes for labeled myosin (Figs 5 and 6) are quite long compared to the correlation times observed for anisotropy decay (discussed below), indicating that molecular reorientation dominates anisotropy decay, and justifying the straightforward analysis used below.

(d) *Anisotropy experiments*

(i) *Triplet–triplet absorption experiments*

Some preliminary experiments with solutions of S-1 and myosin were done on the instrument at Princeton University (Fig. 2), which, because of its time resolution, provided data in the time range of 100 nanoseconds to several microseconds, for direct comparison with the results of the nanosecond fluorescence emission anisotropy experiments of Mendelson *et al.* (1973). The results of triplet–triplet absorption anisotropy experiments are presented in Figure 7. The form of anisotropy decay for S-1 is roughly that of a single exponential that decays to zero; whereas the myosin decay is seen to have at least two components, a shorter one in the range of hundreds of nanoseconds, and a longer, microsecond component. The correlation time estimated from the anisotropy decay curve of S-1 is 250 nanoseconds. For myosin, the correlation time for the faster process is approximately 400 nanoseconds. These correlation times are similar to those observed in time-resolved fluorescence anisotropy experiments (Mendelson *et al.*, 1973), and to effective correlation times obtained by electric birefringence (Kobayasi & Totsuka, 1975) and by e.p.r. (Thomas *et al.*, 1975*a*). The existence of the microsecond decay is evidence that the faster motion in myosin is restricted in amplitude. This phenomenon was examined in detail and is discussed below.

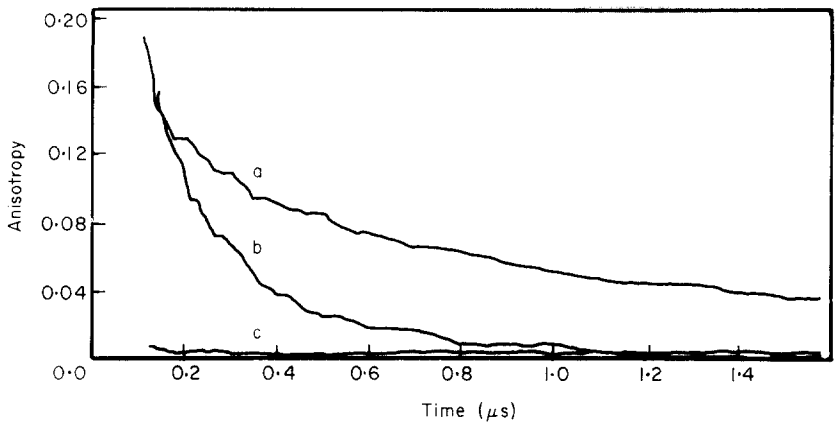

FIG. 7. Time-resolved absorption anisotropy of eosin-labeled myosin and S-1. Triplet–triplet absorption experiments were performed on the instrument shown in Fig. 2. Excitation at 532 nm, approx. 200 μJ/pulse; observed at 632·8 nm. Experiments done at 4°C. Curve a, myosin 8·7 μM (4·0 mg/ml); dye/protein molar ratio 1·2; 0·5 M-NaCl, 1 mM-EDTA, 0·1 mM-DTT, 1 mM-NaN_3, 10 mM-MOPS (pH 7·0). Curve b, S-1 prepared from a 15-min chymotryptic digest of the same labeled myosin: S-1, 3·8 μM (0·43 mg/ml); dye/protein molar ratio 0·52; 120 mM-NaCl, 1 mM-EDTA, 0·1 mM-DTT, 10 mM-MOPS (pH 7·0). Both protein samples had been deoxygenated by dialysis (see Materials and Methods). Samples were not stirred during data acquisition. Curve c, eosin, 25μM in water, bubbled continuously with argon.

(ii) *Singlet absorption and triplet emission experiments*

The remaining experiments were done on the instrument at the University of Minnesota (Fig. 1), where both singlet absorption (ground-state depletion) and triplet emission (phosphorescence) data were obtained over a wider time range. The results of singlet absorption experiments with S-1 and myosin (Fig. 8) confirm and extend the results obtained with the triplet absorption data (Fig. 7).

The initial anisotropies in both S-1 and myosin are at least 0·24 at the earliest observable time (0·1 μs). This implies that motions with correlation times less than 0·1 microsecond reduce $r(t)$ from the fundamental anisotropy r_0 to about 0·24, but that these motions are limited in amplitude. This important result means that eosin covalently bound to myosin is a probe sensitive to macromolecular fluctuations in the microsecond to millisecond range. The theoretical maximum value for r_0 depends on the angle between the transition dipoles of excitation and observation, and thus will differ among the three kinds of experiments reported here (triplet absorption, triplet emission, ground-state depletion). Estimates of r_0 have been obtained (Cherry & Schneider, 1976; Garland & Moore, 1979) for solid solutions of eosin; protein conjugates usually show lower initial anisotropies. In the singlet absorption experiment, the observation wavelength is in the same singlet absorption band as the excitation wavelength, and thus the observed transition dipole is parallel to the photoselected dipole, and r_0 must be close to the theoretical maximum value 0·4. This situation makes the absorption experiments with observation at 488 nm inherently more sensitive.

Experiments on S-1 were performed primarily to determine whether probe

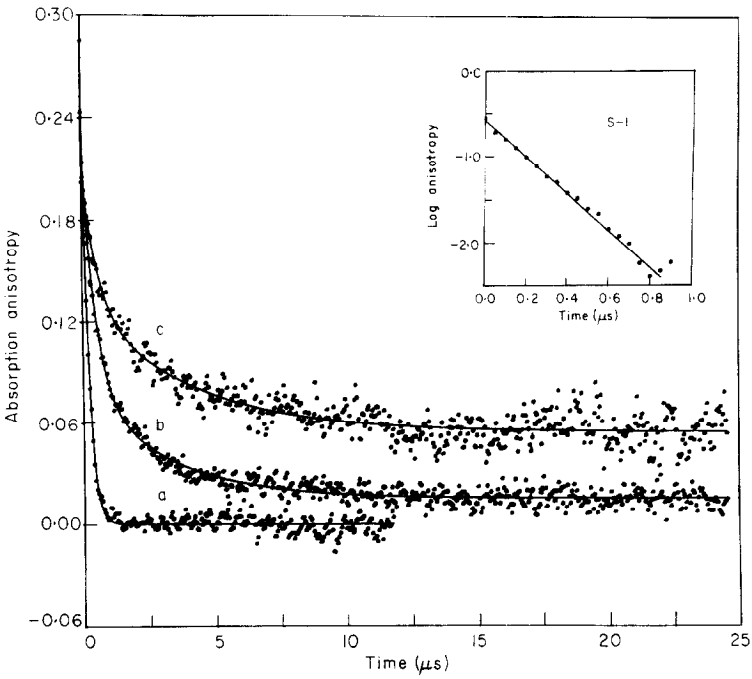

FIG. 8. Absorption anisotropy of S-1, myosin and myosin filaments. Singlet absorption experiments (broadband pulsed excitation centered at 530 nm, continuous wave observation at 488 nm) were done on the instrument shown in Fig. 1(a). Experiments were done at 4°C. The enzymatic deoxygenating system was added; samples were stirred magnetically at about 3 Hz during data acquisition. Curve a, S-1 75·1 μM (8·64 mg/ml); dye/protein molar ratio 0·23; 120 mM-KCl, 5 mM-$MgCl_2$, 1 mM-EDTA, 1 mM-NaN_3, 25 mM-MOPS (pH 7·0). Curve b, myosin 11·9 μM (5·46 mg/ml); dye/protein molar ratio 0·72; 0·5 M-KCl, 5 mM-$MgCl_2$, 1 mM-EGTA, 1 mM-NaN_3, 25 mM-MOPS (pH 7·0). Curve c, myosin filaments, 2·6 mg/ml, prepared by dialysis of labeled myosin in the S-1 buffer given for a. Unbroken lines are the result of a fit of equation (3) to the data in curves b and c, or equation (2) to the data in curve a. The averages of the fitted parameters obtained in several separate experiments are given in Table 2. The inset is an expanded semi-log plot of the anisotropy data for the S-1 from curve a.

attachment is rigid enough to permit the analysis of myosin data in terms of overall head motion. The singlet absorption anisotropy of S-1 in aqueous solution at 4°C follows a single-exponential decay with a correlation time of 208(±14) nanoseconds (Fig. 8 and Table 2). Although these data have less time-resolution (50 ns/point) than that of the triplet absorption data (2 ns/point, Fig. 7), they give essentially the same result. These data, covering at least five correlation times, are consistent with and significantly extend previous fluorescence (singlet emission) data on IAEDANS-1 labeled S-1 (Mendelson *et al.*, 1973), which covered less than one correlation time.

In terms of the theory of rotational diffusion of rigid ellipsoids with a rigidly attached dipolar oscillator (absorption or emission transition dipole), the observed anisotropy decay for S-1 would correspond, for example, to isotropic reorientation of a sphere having a molecular weight about three times that of S-1, or to the reorientation of the long axis of a rather long prolate ellipsoid (axial ratio about 4) with the molecular weight of S-1, in which the transition dipole is approximately parallel to the long axis. This is the interpretation given previously

TABLE 2

Absorption anisotropy decay parameters of S-1, myosin and myosin filaments in solution at 4°C

	A_1† (A_1/r_0)*	ϕ_1 (μs)	A_2 (A_2/r_0)	ϕ_2 (μs)	$A_3 \equiv r_\infty$ (A_3/r_0)	$\sum A_i \equiv r_0$
Subfragment-1	0·288±0·008	0·208±0·014			0·002±0·002	0·29
Myosin	0·14±0·02	0·40±0·17	0·084±0·024	2·6±0·8	0·015±0·001	0·24
	(0·56±0·07)		(0·35±0·07)		(0·060±0·010)	
Myosin filaments	0·080±0·021	0·73±0·13	0·058±0·014	4·9±1·7	0·049±0·005	0·19
	(0·43±0·07)		(0·31±0·05)		(0·26±0·03)	

† Anisotropy decay parameters obtained by fit of equation (2) to S-1 data and of equation (3) to myosin and filament data. Values are given as the average ± the standard deviation ($n = 2$ for S-1, $n = 3$ for myosin, $n = 3$ for filaments) for experiments done on separate samples from the same batch of labeled myosin characterized in Table 1 and Fig. 8. Experiments were done on the instrument shown in Fig. 1(a), with conditions as given for Fig. 8. * Numbers in parentheses have been divided by r_0.

to explain similar long correlation times obtained with the fluorescence probes (Mendelson *et al.*, 1973), or with spin labels (Thomas *et al.*, 1975*a*,*b*). However, the single exponential decay for S-1 (shown more clearly in the inset to Fig. 8) could also correspond to the degenerate correlation times of a fairly asymmetric oblate ellipsoid in which the transition dipole can have almost any orientation (Yang & Wu, 1977; Eads, 1982). The actual shape of the hydrated S-1 particle is not known with certainty, and its degree of hydration is in dispute (Yang & Wu, 1977; Mendelson & Kretzschmar, 1980; Garrigos *et al.*, 1983). Thus analysis in terms of equivalent hydrodynamic ellipsoids, or even more detailed shapes, is uncertain. Unambiguous interpretation of the anisotropy data is not possible without a great deal more information than is available. No matter what model is assumed for the shape of S-1, slow probe motion strongly suggests that the probe is fixed rigidly to S-1, so that the anisotropy decay reports overall motion.

In order to ascertain whether the probe follows overall tumbling of the macromolecule, S-1 was dissolved in a viscous solvent (containing 75% glycerol) and the absorption anisotropy was measured as a function of temperature. If the probe is rigidly bound in the submicrosecond to millisecond range, correlation times should be proportional to the ratio of solvent viscosity to absolute temperature. This approximation does not take into account changes in protein conformation and in the amount of solvent bound that might occur with changes in solvent and temperature. The results are shown in Figure 9. Based on the observed correlation time of 208(±14) nanoseconds at 4°C in water (Fig. 8), S-1 in 75% (w/w) glycerol is predicted to have correlation times ϕ of 25 microseconds at 2·5°C and 10 microseconds at 13·5°C. We obtained 15(±3) microseconds and 7·4(±1·5) microseconds at these temperatures by fitting a single exponential function (eqn (2)) to the data. We consider this to be good agreement, given the approximation and the uncertainty of the values of ϕ.

We also approached the probe-rigidity question by binding heads to actin, which has been shown previously to immobilize probes bound to SH_1 (Thomas *et al.*, 1975*a*). The results are shown in Figure 10, which compares phosphorescence

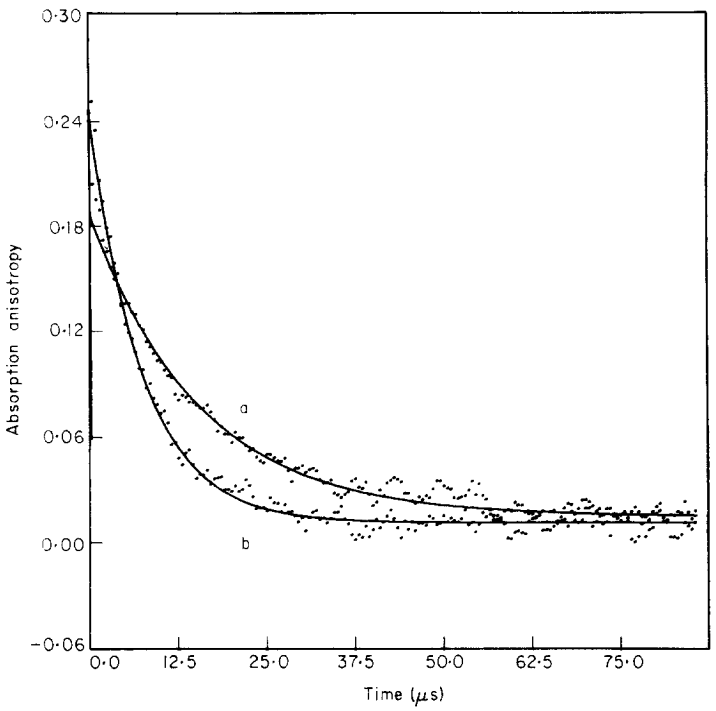

FIG. 9. Temperature-dependence of absorption anisotropy of eosin-labeled S-1 in glycerol. Singlet absorption experiment (broadband pulsed excitation centered at 530 nm, continuous wave observation at 488 nm) performed on the instrument shown in Fig. 1(a). S-1 was prepared from a 15-min digest of eosin-labeled myosin and stored in 50% (w/w) glycerol. This S-1 comes from the same preparation characterized in Table 2 and in Fig. 8. The enzymatic deoxygenating system was added to the S-1 in 50% glycerol; glycerol saturated with argon was added by weight to 75%; the sample was mixed carefully under argon, centrifuged to remove bubbles, and transferred to a cuvette. Final composition was S-1, 34·8 μM (4·00 mg/ml); dye/protein molar ratio 0·23; 30 mM-KCl, 1·25 mM-$MgCl_2$, 0·25 mM-EGTA, 0·25 mM-NaN_3, 6·25 mM-MOPS, 75% (w/w) glycerol. Temperature was monitored continuously with a copper-constantan thermocouple immersed in the sample. The sample was stirred magnetically at about 3 Hz during data acquisition. Curve a, $T = 2·5$°C, curve b, $T = 13·5$°C. Unbroken lines are the results of a least-squares fit to a single exponential function (eqn (1)). Correlation times obtained are 15·3 μs at 2·5°C (curve a) and 7·4 μs at 13·5°C (curve b).

emission anisotropy of actomyosin with that of myosin filaments. (We selected emission in this case since absorption data are, at this time, quite difficult to obtain on actomyosin at these concentrations.) Residual anisotropy was higher in actomyosin; thus depolarizing motions are more restricted in actomyosin, and probe motions decrease when head motions are reduced by binding. This further supports the idea that probe motion in the microsecond range reflects overall motion of myosin heads. The details of the first microsecond of anisotropy decay in actomyosin (not available in emission experiments due to gating requirements) will require experiments with greater time resolution.

We made a detailed comparison of the absorption anisotropy decay in solutions of S-1, myosin and myosin filaments. Typical results of single experiments are shown in Figure 8 and a summary is given in Table 2, which gives the parameters obtained by least-squares fit of the data to one- or two-exponential functions

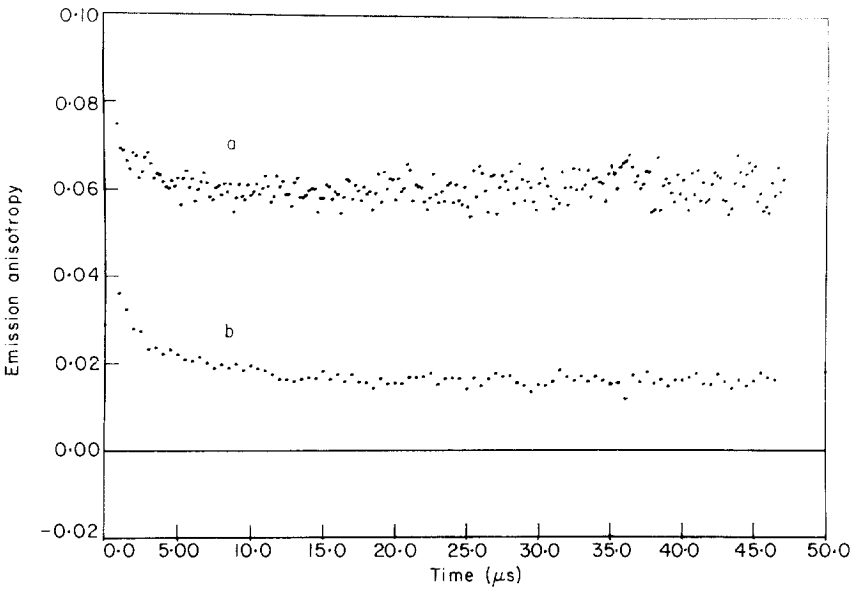

FIG. 10. Phosphorescence emission anisotropy of myosin filaments and actomyosin. Experiments (broadband excitation centered at 530 nm) were done on the instrument shown in Fig. 1(b), at 4°C without stirring. a, Actomyosin (myosin-labeled), 25 μM-actin, 5 μM-myosin, 120 mM-KCl, 5 mM-$MgCl_2$, 1 mM-EGTA, 1 mM-NaN_3, 25 mM-MOPS (pH 7·0); oxygen was displaced by dialysis in a nitrogen-bubbled bath. b, Myosin filaments, 8·22 mg/ml; dye/protein ratio 0·72; buffer as for a, except that the myosin sample contained the deoxygenating enzyme system.

(eqns (2) and (3)). One-exponential functions were not adequate to represent myosin or filament data. This was obvious in superimposed plots of fit and data. Fits of the two-exponential function (no parameters constrained) were good, as judged by inspection, over the entire time range of 50 nanoseconds to 25 microseconds. Thus at least two decay terms and one constant term were required. In contrast, attempts to fit S-1 data to a two-exponential function did not produce satisfactory fits with two significantly different correlation times, and the constant term (A_3) was found to be negligible. Reproducibility was established in experiments on separate samples, as reflected in the standard deviations in Table 2. We found that the anisotropy function for filaments was independent of concentration from 1·5 to 6 mg/ml. A likely explanation for the observation of a constant component of anisotropy is that motions are restricted in rotational amplitude, as analyzed in more detail in the Discussion.

The results of absorption anisotropy experiments at 4°C may be summarized as follows: motion of the probe on S-1 free in solution follows rotational Brownian diffusion of the whole particle, and this motion is characterized by a single correlation time of 208 nanoseconds. Motion of the probe on the head of myosin in solution has short (400 ns) and long (2·6 μs) correlation times, and the anisotropy decays nearly to zero, suggesting that there is a fast motion that is restricted in amplitude, and a slower motion that is slightly restricted. Preliminary results of longer-time measurements on monomers suggest that the anisotropy decays fully to zero within 50 to 100 microseconds. Motion in myosin filaments also has a fast

(submicrosecond) and a slower (microsecond) component; these are roughly twice as slow as the monomer motions, and there is a substantial component of anisotropy that is constant in the 50 microsecond time range, suggesting that both fast and slow motions are fairly restricted in amplitude.

4. Discussion

(a) *Triplet anisotropy applied to rotational motion in muscle proteins*

Fluctuations and repetitive motions occur in the nanosecond to millisecond range in contractile proteins. Changes in the characteristic fluctuations of molecular regions in biological macromolecules may be associated with transitions from one physiological state to another (Gurd & Rothgeb, 1979). For example, in the nanosecond range, the motion of a spin probe at one site on myosin can be strongly affected by the state of a nucleotide at its binding site (Seidel & Gergely, 1973), and mobile protons in S-1 are strongly affected by actin binding (Highsmith *et al.*, 1979). In the microsecond range, saturation transfer e.p.r. results demonstrate that rotational motions of myosin heads change dramatically as muscle fibers go through different physiological states (Thomas *et al.*, 1980; Thomas, 1982). Since transients in muscle-fiber tension and length have been observed in the microsecond time range (Ford *et al.*, 1981; Barden & Mason, 1979), microsecond motions at the molecular level may be found to have a direct relationship to the macroscopic events. Therefore, it is essential to obtain time-resolved and orientation-resolved information about these motions. The requirements for a suitable spectroscopic probe for this task are met by the halogenated xanthene dyes (e.g. eosin and erythrosin), which have long-lived triplet electronic states and can be modified to react with protein functional groups. Triplet probes can extend observation times to milliseconds and provide time resolution, complementing the fluorescence and e.p.r. methods, respectively.

In the present study we have used eosin-5-iodoacetamide to label myosin site-specifically at the reactive sulfhydryl, SH_1, in the head region. Evidence from absorption and emission spectra, and from phosphorescence emission lifetimes, suggests that the probe is partly buried in the protein. High initial anisotropies at early times (50 ns) demonstrate that the probe is bound rigidly enough to monitor submicrosecond and slower motions with good sensitivity. The anisotropy decays at early times in S-1 and in myosin monomers agree with the results from other methods. The presence of microsecond decay components in myosin monomers and filaments, and of a residual anisotropy in filaments, represent new information in a time range that was previously inaccessible. We conclude that myosin head motion in the hundreds of nanoseconds range is not isotropic but, rather, somewhat restricted in amplitude, and that both fast (nanosecond) and slow (microsecond) head motion in filaments occur in a restricted angular range.

(b) *Analysis of residual anisotropy*

An important model-independent result of anisotropy theory is that the ratio of residual anisotropy to the initial anisotropy is equal to the square of the order

parameter, S, which, for a dipolar probe, is the square of the expectation value of the second Legendre polynomial of $\cos\theta$, $P_2(\cos\theta)$. Here θ is the angle that the observed transition dipole makes the axis established by the polarization of the photoselection pulse:

$$r_\infty/r_0 = S^2 = \langle P_2(\cos\theta)\rangle^2. \quad (4)$$

(e.g. see Lipari & Szabo, 1980). In myosin filaments under the conditions studied, this ratio was non-zero, hence the square of order parameter is non-zero, suggesting that heads sample a range of angles $\Delta\theta$ less than 180°. Extraction of further information from the order parameter requires a geometrical model so that the average can be evaluated. For physically intuitive reasons, we chose the wobbling-in-a-cone model (Kinosita *et al.*, 1977). Within this framework, the ratio r_∞/r_0 can be evaluated in terms of the cone half-angle θ_c:

$$r_\infty/r_0 = [\tfrac{1}{2}\cos\theta_c(1+\cos\theta_c)]^2. \quad (5)$$

Results of this analysis are given in the sixth column of Table 3, which shows that in filaments head motion is somewhat restricted. The value of 102° for the full cone angle ($2\times\theta_c$) agrees with the conclusion from e.p.r. studies of myosin head disorder in relaxed or stretched muscle fibers, that angular amplitudes exceed 90° (Thomas & Cooke, 1980; Barnett & Thomas, 1984). The small residual anisotropy of myosin in the observed time range indicates that motions in this range may also be slightly restricted.

The above analysis assumes that the data in Table 2 reflect directly the motions of probes on myosin heads, which amounts to assuming that r_∞ is the same for the probes on rods (2·3(±1)% of the total probes) as for the probes on heads. In fact, probes on rods could have r_∞ values ranging from zero to r_0. Thus, assuming that r_0 is the same for probes on rods and heads, the values of r_∞/r_0 due specifically to probes on *heads* could be greater or less than the values in Table 2 by 0·023±0·01. If this additional uncertainty were taken into account, the result would be to increase the uncertainty of θ_c (Table 3, last column) for monomers by 5° ($\theta_c = 69(\pm 7)°$) and for filaments by 2° ($\theta_c = 51(\pm 4)°$. Similarly small additional uncertainties would apply to the other parameters in Table 3.

TABLE 3

Restricted diffusion of myosin heads (wobbling in a cone model)

	Faster component		Slower component		Overall motion
System	θ_c (°)	D_w (s^{-1})	θ_c (°)	D_w (s^{-1})	θ_c (°)
Myosin monomer	42±4	$3{\cdot}6\times10^5$	59±4	$8{\cdot}3\times10^4$	69
Myosin filament	34±4	$1{\cdot}8\times10^5$	40±4	$2{\cdot}6\times10^4$	51

Half-angle of diffusion, θ_c, and wobbling diffusion coefficients, D_w, obtained from absorption anisotropy data (Table 2) according to Kinosita *et al.* (1977) and as described in the text. The values in the last column assume wobbling in a single cone (section (b)) while those in other columns assume two cones (section (c)).

(c) *Analysis of rates and amplitudes of head motion in terms of more specific models*

Observation of two correlation times can be explained in terms of either diffusion of a probe that makes an angle much greater than 0° with the major axis of an elongate rigid body, or in terms of restricted motion in a segmentally flexible molecule. We consider first the rather implausible idea that myosin is a rigid body in which the labeled heads are both at some fixed angle with the rod. The motion at times much shorter than the correlation time for end-over-end tumbling is that of a symmetrical top. When we apply the theory for such motion (Kinosita & Kawato, 1981) we find that the two observed correlation times have roughly the correct ratio, but that the ratios of amplitudes do not agree at all with the theory.

Next we consider a segmented molecule with free swivels at segment junctions. The theory (Wegener, 1982) predicts single exponential decay of anisotropy if the observed dipole is parallel to the long axis of S-1 or complex decay if the dipole makes an angle with the long axis. In either case, the slow microsecond components that we observe are not predicted, and the faster components we observe are much slower than predicted.

A segmented molecule with restricted motion at one swivel would produce complex anisotropy, with the early component of the decay corresponding to apparently unrestricted motion, and the late component corresponding to overall tumbling (Wegener, personal communication). This is also inconsistent with our results, which show an early component twice as slow as expected, and a second component that is only about one tenth as slow as expected for overall tumbling, which is calculated (Garcia de la Torre & Bloomfield, 1980) or observed (Rosser *et al.*, 1978; Bernengo & Cardinaud, 1982) to be in the 16 to 40 microsecond range.

We finally analyzed the data in terms of rates and amplitudes of motion of a segment of a molecule with two swivels, by extension of the cone model of Kinosita *et al.* (1977). We treated separately the fast and slow components of anisotropy decay in myosin monomer and in filaments. We assume that the two well-separated (by a factor of about 7) correlation times represent independent motions, each of which can be treated by the cone model. For each component, an expression for the anisotropy as a function of time is obtained as an infinite sum of exponentials, which can be approximated closely by the simple expression:

$$r(t) = (r_0 - r_\infty) \exp(-t/\phi) + r_\infty, \tag{6}$$

where ϕ is an effective correlation time related to the "wobbling" diffusion coefficient by the expression:

$$D_w = \langle \sigma \rangle / \phi. \tag{7}$$

Here $\langle \sigma \rangle$ is a function of the cone half-angle. The angle is obtained from equation (5), by taking for r_0 and r_∞ the respective values $(A_1 + A_2 + A_3)$ and $(A_2 + A_3)$ for the fast motion, or $(A_2 + A_3)$ and A_3 for the slow motion, where A_1, A_2 and A_3 are from equation (3) and Table 2. The diffusion coefficients D_w were estimated from the values of ϕ_i (Table 2) by the procedure of Kinosita *et al.*

(1977). The results of this analysis are given in Table 3. From this we deduce that the faster motion has a slightly smaller amplitude (θ_c) in filaments (34°) than in monomers (42°), and the rate (D_w) in filaments is only twice as slow. On the other hand, the slower motion has a 50% smaller amplitude in filaments ($\theta_c = 40°$) than in monomer ($\theta_c = 59°$), and the rate in filaments is three times slower. Our use of Figure 3 of Kinosita *et al.* (1977) implicitly assumes that the observed transition dipole is parallel to the molecular axis that reorients in the cone. Although, as discussed above, the S-1 data suggest that this assumption is valid, we cannot rule out other probe orientations. However, even in the case where the probe axis is perpendicular to the molecular axis, the rates and amplitudes deduced by the theory are roughly similar to those deduced from the assumption that the axes are parallel.

Analysis used to construct Table 3 was suggested by the nature of the data and by our present knowledge of myosin structure. It seems quite plausible that *the faster motions are due to flexibility at the junction between S-1 and S-2, and the slower ones are due to flexibility at the junction between S-2 and light meromyosin.* Restrictions in motion might be due to steric constraints near the points of flexibility or to collisions of heads with each other. One particularly attractive picture for head motion in filaments is a simple two-state model corresponding to the S-1 plus S-2 region (1) attached to or (2) released from the thick filament backbone. Motion in the released state is considered to be less restricted. The residual anisotropy would be due, in part, to the attached population. Our data are certainly consistent with such a model, and several experiments are immediately suggested to test it. Other models might account for the observations: such as restricted torsional motion or slow internal fluctuations. That other possibilities exist should not obscure the most important model-independent conclusion: nanosecond and microsecond rotational motions of myosin heads in filaments are moderately restricted in amplitude.

(d) *Relationship to other work*

The power of the triplet anisotropy technique is illustrated well by comparison with results from other studies of rotational motion of labeled myosin heads in myosin filaments. Fluorescence anisotropy data, limited by short excited-state lifetimes to a time range of only 200 nanoseconds, could be used only to estimate the *initial* decay rate and could not include either the slower (microsecond) decay component or the non-zero residual anisotropy (Mendelson *et al.*, 1973; Mendelson & Cheung, 1976,1978). The observation that the initial decay was slower in filaments than in monomers was consistent with a decrease in *either* the rate (diffusion coefficient) or amplitude (θ_c) or *both*. Those workers chose to assume that the diffusion coefficient remained unchanged. The result was the suggestion that myosin head motion is quite restricted (half cone angle less than 20°). With a complete data set for a triplet probe at the same site, we verify that the initial anisotropy decay rate is less in filaments, but the non-zero residual anisotropy shows that this is due to decreases in *both* diffusion coefficient and amplitude.

Thus the amplitude of motion is considerably greater than suggested previously. The only previous attempt to measure both rates and amplitudes of microsecond head motion employed e.p.r. of spin-labeled myosin. These experiments did provide (1) evidence for microsecond motion in myosin filaments (Thomas *et al.*, 1975*a*; using s.t.-e.p.r.) and (2) evidence that the total angular range of myosin head motions was greater than 90° in relaxed or stretched muscle fibers (Thomas & Cooke, 1980; Barnett & Thomas, 1984; using conventional e.p.r.), consistent with the present results. However, the lack of time-resolution in e.p.r. precluded a detailed analysis in terms of individual motional components. The ten microsecond effective correlation time for head motion in filaments from s.t.-e.p.r. was obtained by comparison of the observed lineshape to a reference spectrum that assumes isotropic motion. This procedure has now been found to overestimate the restricted motion, and the use of such reference spectra shows that the s.t.-e.p.r. data for myosin filaments are consistent with the anisotropy data reported here (Barnett & Thomas, 1984; Lindahl & Thomas, 1982). Thus the optical results can be used to refine analysis of e.p.r.-spectra.

The disposition of the region containing S-1 and S-2 relative to the thick filament backbone has been studied using proteolytic susceptibility and crosslinking kinetics (Ueno & Harrington, 1981; Reisler *et al.*, 1983; Sutoh *et al.*, 1978). These workers interpret relatively slow rates of proteolysis and relatively fast rates of crosslinking to correspond to compact association of S-1, S-2 or light meromyosin with the thick filament backbone. Our observation of microsecond reorientation in filaments (pH 7·0) suggests that considerable freedom of motion of some heads, or somewhat restricted motion of all heads, persists even when the chemical reactivity is relatively low. Dynamic light-scattering results (Suzuki & Wada, 1981; Kubota *et al.*, 1983; Chu *et al.*, 1984) also show that some hydrodynamic modes may correspond to an open, fluctuating structure of the region containing S-1 and S-2. The proximity of heads and S-2 to the thick filament backbone (deduced from proteolysis and crosslinking) appears to change with intensive variables such as pH, ionic strength, divalent cation concentration, and the presence of nucleotides (Morimoto & Harrington, 1974; Ueno & Harrington, 1981; Reisler *et al.*, 1983). The triplet anisotropy method is applicable to the study of the relationship between such effects and the molecular dynamics.

In order to obtain a less-ambiguous molecular interpretation of time-resolved anisotropy data, more theoretical and experimental work must be done. In particular, the theoretical methods for motion in segmented molecules will have to incorporate the effects of restrictions to motion. More precise information about the shape of myosin (especially S-1), and data on probes at *several* specific sites within this structure, will greatly facilitate this analysis.

In a natural extension of our work with myosin, we have recently achieved good labeling specificity of myosin heads in glycerinated fibers (unpublished results). Thus we will be able to ask whether the motions detected in synthetic myosin filaments in the present study are comparable to those observed in the native filament lattice, as suggested by recent e.p.r. results (Barnett & Thomas, 1984). The triplet anisotropy method promises to become a powerful tool in orientation and time-resolved studies of myofibrillar components during

transitions among physiological states of muscle fibers, especially during contraction.

We acknowledge the valuable and ingenious contributions of Robert H. Bennett and Dr Brian P. Citak, who designed and assembled the electronics and the interface software for the time-resolved spectrometers; Kerry Lindahl, James Lietch, Joseph Stone and Joel Schneider for data-processing software development; and David Momont for development of gel and densitometry methods. This work was supported by grants from the National Institutes of Health (GM27906, AM32961 and RR01439 to D.D.T. and GM30789 to R.H.A.), and to D.D.T. from the American Heart Association (80-850), the National Science Foundation (PCM8004612), and the Muscular Dystrophy Association of America. D.D.T. was supported by a Research Career Development Award from the National Institutes of Health, and is currently supported by an Established Investigatorship from the American Heart Association.

REFERENCES

Austin, R. H., Chan, S. S. & Jovin, T. M. (1979). *Proc. Nat. Acad. Sci., U.S.A.* **76**, 5650–5654.

Badea, M. G. & Brand, L. (1979). *Methods Enzymol.* **61**, 378–425.

Barden, J. A. & Mason, P. (1978). *Science*, **199**, 212–213.

Barnett, V. B. & Thomas, D. D. (1984). *J. Mol. Biol.* **179**, 83–102.

Bernengo, J. C. & Cardinaud, R. (1982). *J. Mol. Biol.* **159**, 501–507.

Brand, L., Ross, J. B. A. & Laws, W. R. (1981). *Ann. N.Y. Acad. Sci.* **366**, 197–207.

Burkli, A. & Cherry, R. J. (1981). *Biochemistry*, **20**, 138–143.

Cherry, R. J. (1979). *Methods Enzymol.* **54**, 47–61.

Cherry, R. J. & Schneider, G. (1976). *Biochemistry*, **15**, 3657–3661.

Cherry, R. J., Cogoli, A., Oppliger, M., Schneider, G. & Semonza, G. (1976). *Biochemistry*, **15**, 3653–3656.

Chu, B., Fan, S. F., Dewey, M. M., Gaylinn, B., Colflesh, D. & Greguski, R. (1984). *Biophys. J.* **45**, 253a.

Cooke, R., Crowder, M. S. & Thomas, D. D. (1982). *Nature (London)*, **300**, 776–778.

Cross, A. J., Waldeck, D. H. & Fleming, G. R. (1983). *J. Phys. Chem.* **78**, 6455–6467.

Eads, T. M. (1982). Ph.D. dissertation, Florida State University, Tallahassee.

Eads, T. M. & Mandelkern, L. (1984). *J. Biol. Chem.* In the press.

Fisher, G. J., Lewis, C. & Madill, D. (1976). *Photochem. Photobiol.* **24**, 223–228.

Ford, L. E., Huxley, A. F. & Simmons, R. M. (1981). *J. Physiol.* **311**, 219–249.

Garcia de la Torre, J. & Bloomfield, V. A. (1980). *Biochemistry*, **19**, 5118–5123.

Garland, P. B. & Moore, C. H. (1979). *Biochem. J.* **183**, 561–572.

Garrigos, M., Morel, J. E. & Garcia de la Torre, J. (1983). *Biochemistry*, **22**, 4961–4969.

Godfrey, J. E. & Harrington, W. F. (1970). *Biochemistry*, **9**, 886–893.

Gurd, F. R. N. & Rothgeb, T. M. (1979). *Advan. Protein Chem.* **33**, 73–165.

Harrington, W. F. & Burke, M. (1972). *Biochemistry*, **11**, 1448–1455.

Harrington, W. F. & Himmelfarb, S. (1972). *Biochemistry*, **11**, 2945–2952.

Highsmith, S., Akasaka, K., Konrad, M., Goody, R., Holmes, K., Wade-Jardetzky, N. & Jardetzky, O. (1979). *Biochemistry*, **18**, 4238–4244.

Highsmith, S., Wang, C. C., Zero, K., Pecora, R. & Jardetzky, O. (1982). *Biochemistry*, **21**, 1192–1197.

Horie, T. & Vanderkooi, J. M. (1981). *Biochim. Biophys. Acta*, **670**, 294–297.

Huxley, H. E. (1969). *Science*, **164**, 1356–1366.

Huxley, H. E. (1975). *Acta Anat. Nippon*, **50**, 301–325.

Huxley, H. E. & Haselgrove, J. C. (1976). In *Myocardial Failure*, pp. 4–15, Springer, Berlin.

Huxley, H. E., Faruqi, A. R., Kress, M., Bordas, J. & Koch, M. H. J. (1982). *J. Mol. Biol.* **158**, 637–684.

Hvidt, S., Nestler, F. H. M., Greaser, M. L. & Ferry, J. D. (1982). *Biochemistry*, **21**, 4064–4073.
Hyde, J. S. & Thomas, D. D. (1980). *Annu. Rev. Phys. Chem.* **31**, 293–317.
Jovin, T. M., Bartholdi, M. & Vaz, W. L. C. (1981). *Ann. N.Y. Acad. Sci.* **366**, 176–196.
Kasche, V. & Lindqvist, L. (1965). *Photochem. Photobiol.* **4**, 923.
Kielley, W. W. & Bradley, L. B. (1965). *J. Biol. Chem.* **218**, 653–659.
Kinosita, K. Jr & Kawato, S. (1981). *Biophys. J.* **36**, 277–296.
Kinosita, K. Jr, Kawato, S. & Ikegami, A. (1977). *Biophys. J.* **20**, 289–305.
Kobayasi, S. & Totsuka, T. (1975). *Biochim. Biophys. Acta*, **376**, 375–385.
Kouyama, T. & Mihashi, K. (1980). *Eur. J. Biochem.* **105**, 279–287.
Kubota, K., Chu, B., Fan, S. F., Dewey, M. M., Brink, P. & Colflesh, D. E. (1983). *J. Mol. Biol.* **166**, 329–340.
Lanzettz, P. A., Alvarez, L. J., Reinach, P. S. & Candia, O. A. (1979). *Anal. Biochem.* **100**, 95–97.
Lindahl, K. M. & Thomas, D. D. (1982). *Biophys. J.* **37**, 71a.
Lipari, G. & Szabo, A. (1980). *Biophys. J.* **30**, 489–506.
Lowey, S., Slayter, H. S., Weeds, A. G. & Baker, H. (1969). *J. Mol. Biol.* **42**, 1–29.
Margossian, S. S. & Lowey, S. (1973). *J. Mol. Biol.* **74**, 301–312.
Mendelson, R. A. & Cheung, P. (1976). *Science*, **94**, 190–192.
Mendelson, R. A. & Cheung, P. H.-C. (1978). *Biochemistry*, **17**, 2139–2148.
Mendelson, R. A. & Kretzschmar, K. M. (1980). *Biochemistry*, **19**, 4103–4108.
Mendelson, R. A., Morales, M. F. & Botts, J. (1973). *Biochemistry*, **12**, 2250–2255.
Mendelson, R. A., Putnam, S. & Morales, M. F. (1975). *J. Supramol. Struct.* **3**, 162–168.
Morimoto, K. & Harrington, W. F. (1974). *J. Mol. Biol.* **88**, 693–709.
Reisler, E., Liu, J. & Cheung, P. (1983). *Biochemistry*, **22**, 4954–4960.
Rosser, R. W., Nestler, F. H. M., Schrag, J. L., Ferry, J. D. & Greaser, M. (1978). *Macromolecules*, **11**, 1239–1242.
Seidel, J. C. & Gergely, J. (1973). *Arch. Biochem. Biophys.* **158**, 853–863.
Sutoh, K., Chiao-Chen, Y. C. & Harrington, W. F. (1978). *Biochemistry*, **17**, 1234–1239.
Suzuki, N. & Wada, A. (1981). *Biochim. Biophys. Acta*, **670**, 408–420.
Thomas, D. D. (1978). *Biophys. J.* **24**, 439–462.
Thomas, D. D. (1982). In *Mobility and Function in Proteins and Nucleic Acids, Ciba Foundation Symp. 93*, pp. 169–185, Pitman, London.
Thomas, D. D. & Cooke, R. (1980). *Biophys. J.* **32**, 891–906.
Thomas, D. D., Seidel, J. C., Hyde, J. S. & Gergely, J. (1975*a*). *Proc. Nat. Acad. Sci., U.S.A.* **72**, 1729–1733.
Thomas, D. D., Seidel, J. C., Hyde, J. S. & Gergely, J. (1975*b*). *J. Supramol. Struct.* **3**, 376–390.
Thomas, D. D., Seidel, J. C. & Gergely, J. (1979). *J. Mol. Biol.* **132**, 257–273.
Thomas, D. D., Ishiwata, S., Seidel, J. C. & Gergely, J. (1980). *Biophys. J.* **3**, 873–890.
Thomas, D. D., Wendt, C. H., Francisz, W. & Hyde, J. S. (1983). *Biophys. J.* **43**, 131–135.
Ueno, H. & Harrington, W. F. (1981). *Proc. Nat. Acad. Sci., U.S.A.* **78**, 6101–6105.
Weeds, A. G. & Pope, B. (1977). *J. Mol. Biol.* **111**, 129–157.
Weeds, A. G. & Taylor, R. S. (1975). *Nature (London)*, **257**, 54–56.
Wegener, W. A. (1982). *Biopolymers*, **21**, 1049–1080.
Weltman, J. K., Szaro, R. P., Frackelton, A. R. Jr, Dowben, R. M., Bunting, J. R. & Cathou, R. E. (1973). *J. Biol. Chem.* **248**, 3173–3177.
Yagi, N., O'Brien, E. J. & Matsubara, I. (1981). *Biophys. J.* **33**, 121–138.
Yamaguchi, M. & Sekine, T. (1973). *J. Biochem. (Tokyo)*, **59**, 24–33.
Yang, J. T. & Wu, C. C. (1977). *Biochemistry*, **16**, 5785–5789.

Edited by H. E. Huxley